Supporting Information

Two-dimension MXene Nanosheets on Nano-scale Fibrils in Hierarchical Porous Structure to Achieve Ultra-high Sensitivity

Bingjie Wu[1, 4], Zhenghui Xie[1], Qiwu Shi[2], Junlong Yang[1], Chul B. Park[1, 3], Pengjian Gong[1*] and Guangxian Li[1]

1. *College of Polymer Science and Engineering, State Key Laboratory of Polymer Materials Engineering, Sichuan University, 24 Yihuan Road, Nanyiduan, Chengdu, Sichuan, People's Republic of China, 610065*
2. *College of Materials Science and Engineering, Sichuan University, 24 Yihuan Road, Nanyiduan, Chengdu, Sichuan, People's Republic of China, 610065*
3. *Microcellular Plastics Manufacturing Laboratory, Department of Mechanical and Industrial Engineering, University of Toronto, 5 King's College Road, Toronto, Ontario, Canada, M5S 3G8*
4. *Jiangsu JITRI Advanced Polymer Materials Research Institute, Tengfei Building, 88 Jiangmiao Road, Jiangbei New District, Nanjing, Jiangsu, People's Republic of China, 211800*

* Corresponding author: Pengjian Gong. Email address: pgong@scu.edu.cn. Tel: +86 (028) 8540-1841

Figure S1 Stable MXene colloidal with Tyndall effect

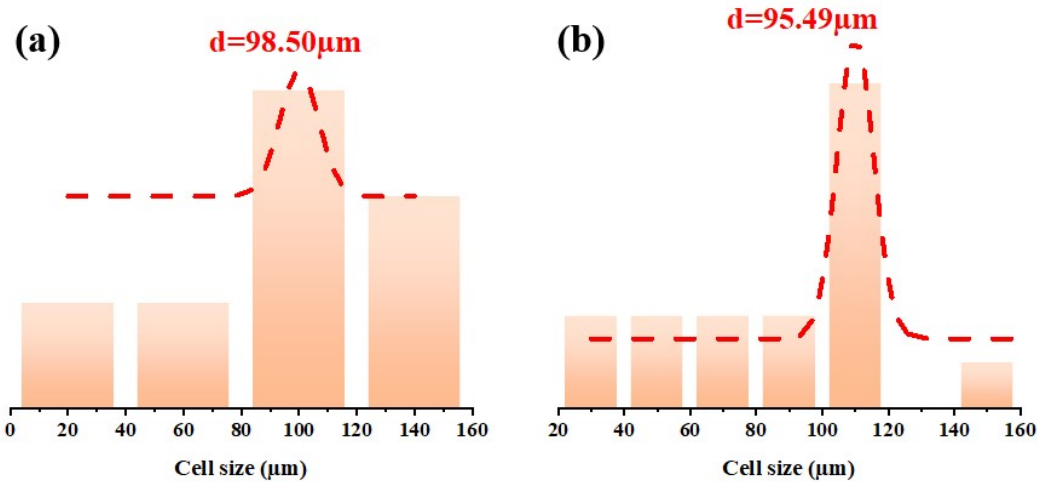

Figure S2 Statistical average cell size for commercial foam skeleton frequently used for piezoresistive sensor whose electrically conductive component was MXene: (a) polyurethane-based skeleton [1]; (b) melamine-based skeleton [2]

Figure S2 shows the statistical average cell size of commercial foam skeleton (polyurethane-based [1] and melamine-based [2] skeletons) used for piezoresistive sensor, and both cases are near 100 μm, too large to effectively take the advantages of two-dimension (2D) MXene nanosheets, while the cell size of EVOH hierarchical skeleton in this work is only 55 μm. The much smaller pore size in the fabricated EVOH hierarchical skeleton is in favor of more contact within the deformed skeleton even under slight pressure and hence significantly improves the piezoresistive sensitivity.

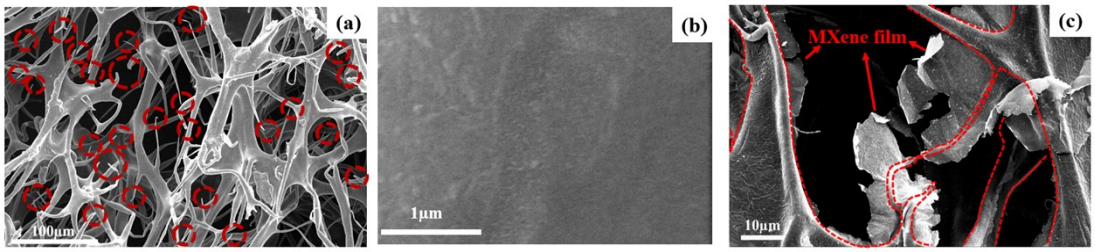

Figure S3 (a) SEM micrographs of EVOH-*g*-EOPO skeleton with many broken fibrils; (b) smooth surface of a micro-sized fibril and (c) membrane-like MXene film among adjacent fibrils (MXene aqueous solution with a concentration of 4 mg/mL)

* Fibril broken ends in (a) are marked in red circle and fibril edges covered by MXene film in (c) are marked by red dotted line.

Large amount of broken fibrils were observed in EVOH-*g*-EOPO skeleton as shown Figure S3 (a). The micro-scale fibrils have smooth surface before assembling 2D MXene nanosheets as shown in Figure S3 (b). For the skeleton assembled in 4 mg/mL MXene aqueous solution, membrane-like MXene film among adjacent fibrils were observed as shown in Figure S3 (c) due to the too many stacked MXene nanosheets.

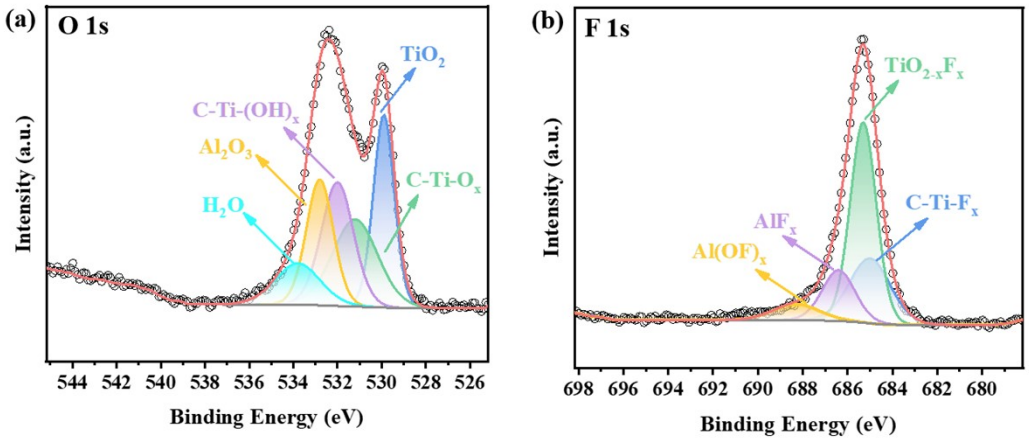

Figure S4 Deconvoluted high-resolution XPS spectrum of MXene for (a) O 1s and (b) F 1s

As shown in Figure S4, The O 1s and F 1s spectrums in Figure S4 imply that a variety of functional groups including -OH, -F, -O, etc. exit on the surface of 2D MXene nanosheets [3].

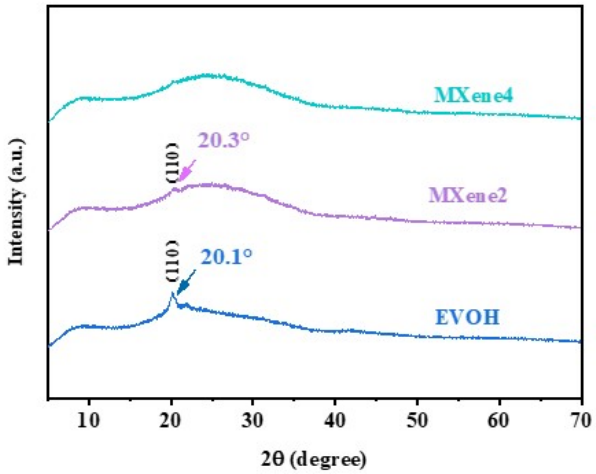

Figure S5 XRD patterns of EVOH, MXene2 and MXene4

It is noted from Figure S5 that the EVOH crystal structure was not affected when 2D MXene nanosheets assembled on the hierarchical skeleton. At a very high MXene concentration in its aqueous solution (for instance, 4 mg/mL), the assembled 2D MXene nanosheets might block the X-ray signal from detecting the EVOH crystal structure in the hierarchical skeleton and then the diffraction peak disappeared.

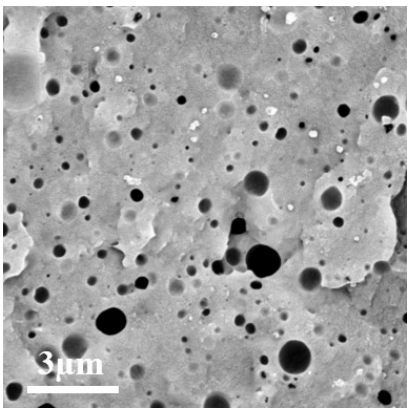

Figure S6 SEM micrograph of phase morphology in EVOH-*g*-EOPO matrix

N,N-dimethylformamide was used to etch EOPO phase in EVOH-*g*-EOPO matrix to reveal the micro-phase separated phase morphology, as shown in Figure S6.

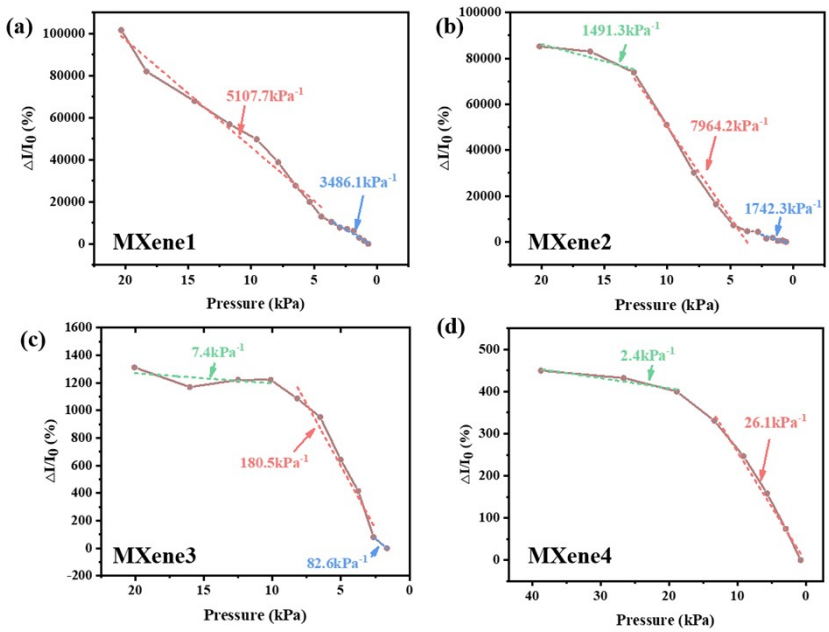

Figure S7 $\Delta I/I_0$-pressure curves for MXene assembled complex hybrid nanostructure in the unloading process: (a) MXene1; (b) MXene2; (c) MXene3; (d) MXene4

As shown in Figure S7, during the unloading process, the variation trend of sensitivity is consistent with the loading process. At the highest sensitivity stage, the sensitivity of MXene1 and MXene2 is also much higher than that of MXene3 and MXene4, showing the similar trend of increasing first and then decreasing. And it is worth noting that the sensitivity during unloading also remains an ultra-high level.

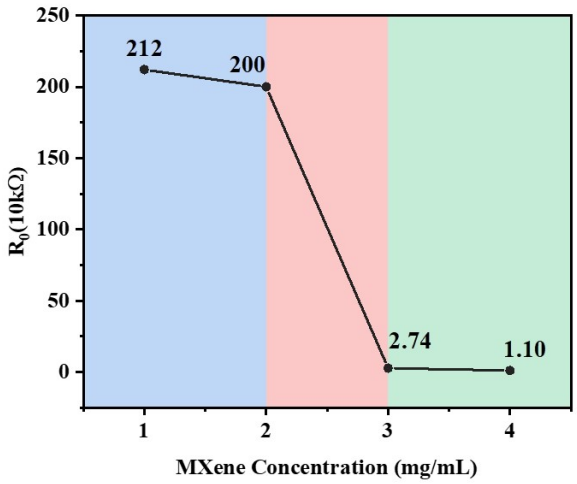

Figure S8 The initial electrical resistance before compressing for MXene1-4 with 1 – 4 mg/mL MXene concentration

The initial electrical resistance before compressing for MXene1 (1 mg/mL),

MXene2 (2 mg/mL), MXene3 (3 mg/mL) and MXene4 (4 mg/mL) is shown in Figure S8. It is obviously observed that the initial electrical resistance of MXene1 and MXen2 is much higher than MXene3 and MXen4. When the MXene concentration exceeds 2 mg/mL, the initial resistance decreases significantly. Therefore, MXene2 is indeed near the percolation.

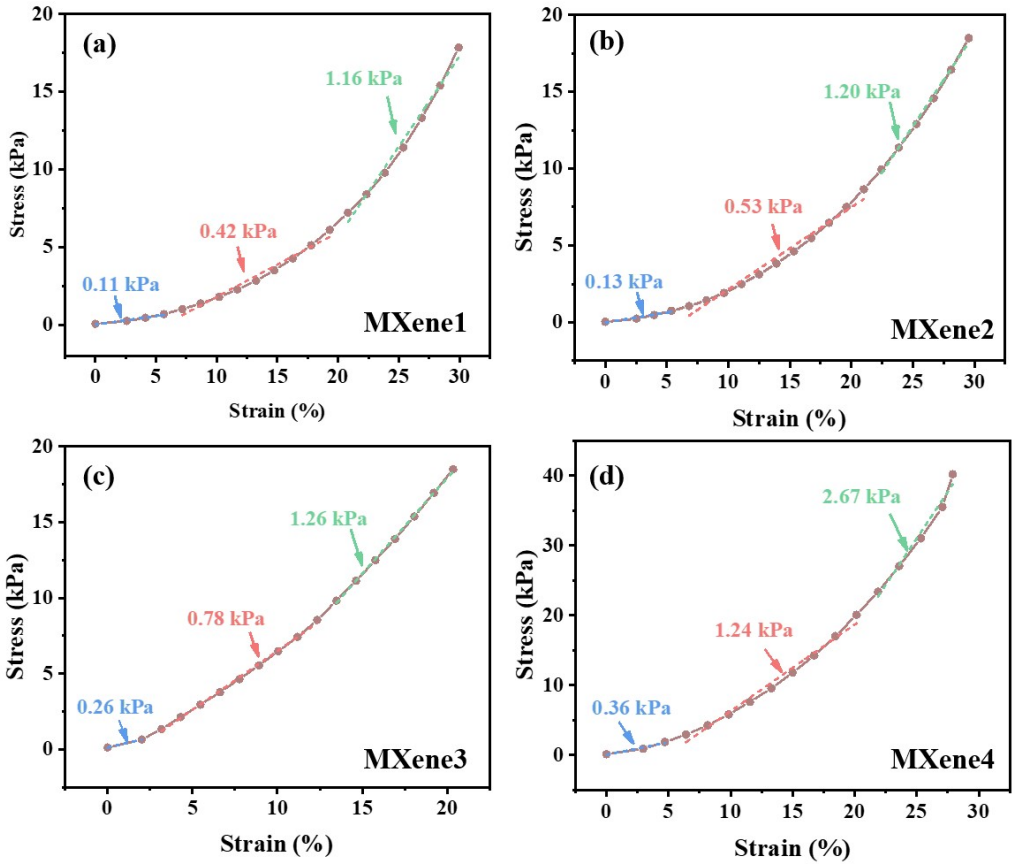

Figure S9 Stress-strain curves of MXene assembled complex hybrid nanostructure with different MXene concentration: (a) MXene1 (1 mg/mL); (b) MXene2 (2 mg/mL); (c) MXene3 (3 mg/mL); (d) MXene4 (4 mg/mL)

The stress-strain curves of MXene assembled complex hybrid nanostructure with different MXene concentration is shown in Figure S9. It can be seen that the modulus of MXene assembled complex hybrid nanostructure rises as the concentration of MXene increases, which is attributed to the mechanical enhanced effect from MXene assembled on the EVOH-*g*-EOPO skeleton. Moreover, from the stress-strain curves, it is noted that as the stress increases, the modulus of MXene assembled complex hybrid nanostructure rises step by step. Three stages can be observed, corresponding to the three stages of the sensing sensitivity: (1) At the first small-stress stage (blue color), the cell of the hybrid nanostructure deforms slightly and there were still large amount

of air in this material and hence the modulus was the lowest; (2) In the second middle-stress stage (red color), the cell of the hybrid nanostructure deforms obviously under compression and contacts with each other, resulting in an increased modulus; (3) In the third large-stress stage (green color), the cell of the hybrid nanostructure has been fully compacted and little air remains and hence the modulus is further improved by continuing to increase the stress. These changes of mechanical properties can better visualize the changes of piezoresistive sensitivity during compression.

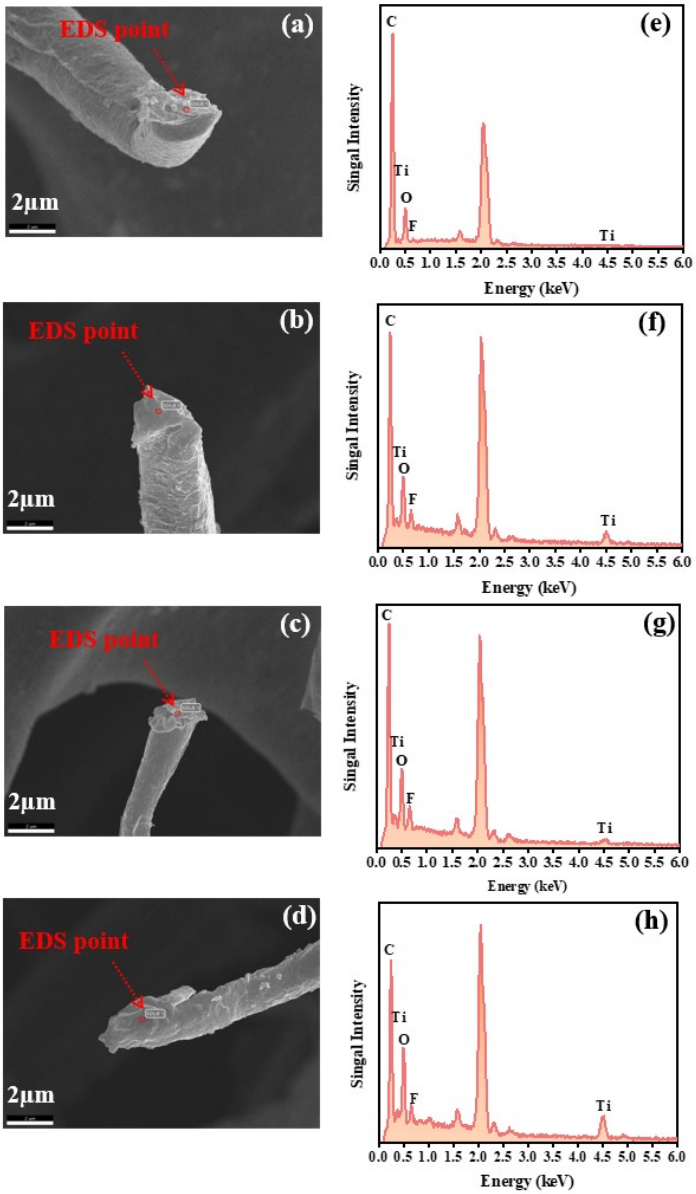

Figure S10 SEM micrograph of MXene covered fibril broken end (a - d) and the corresponding EDS element mapping (e - h) with different MXene samples: (a) and (e) for MXene1; (b) and (f) for MXene2; (c) and (g) for MXene3; (d) and (h) for MXene4

The more experiment evidences of broken fibril covered by MXene nanosheets

are shown in Figure S10. The SEM characterized region is randomly chosen in the whole region of MXene sensor sample. It can be seen that the fracture surface of broken fibril is rough and Ti and F elements are detected by EDS, indicating that all of these broken fibrils are fully covered by MXene nanosheets. Therefore, the MXene covered broken fibril is widely existed in MXene assembled complex hybrid nanostructure and contributes to enhancing the piezoresistive sensitivity.

REFERENCE

1. X. P. Li, Y. Li, X. F. Li, D. K. Song, P. Min, C. Hu, H. B. Zhang, N. Koratkar and Z. Z. Yu, *Journal of Colloid and Interface Science*, 2019, **542**, 54-62.
2. K. Chang, L. Li, C. Zhang, P. Ma, W. Dong, Y. Huang and T. Liu, *Composites Part A-Applied Science and Manufacturing*, 2021, **151**, 106671-106679.
3. T. Feng, W. Huang, H. Zhu, X. Lu, S. Das and Q. Shi, *ACS Applied Materials & Interfaces*, 2021, **13**, 10574-10582.